A study of the Group 1 metal tetra-aza macrocyclic complexes $[M(Me_4cyclen)(L)]^+$ using electronic structure calculations

Hanusha Bhakhoa,[1] Lydia Rhyman,[1,2] Edmond P. Lee,[3,4] Daniel K. W. Mok,[4] Ponnadurai Ramasami[1,2*] and John M. Dyke[3*]

[1]Computational Chemistry Group, Department of Chemistry, University of Mauritius, Réduit 80837, Mauritius
[2]Department of Applied Chemistry, University of Johannesburg, Doornfontein 2028, South Africa
[3]School of Chemistry, University of Southampton, Southampton SO17 1BJ, UK
[4]Department of Applied Biology and Chemical Technology, The Hong Kong Polytechnic University, Hung Hom, Kowloon, Hong Kong

Corresponding Author(s)
*E-mails: p.ramasami@uom.ac.mu (P.R.); jmdyke@soton.ac.uk (J.M.D.)

Graphical Abstract

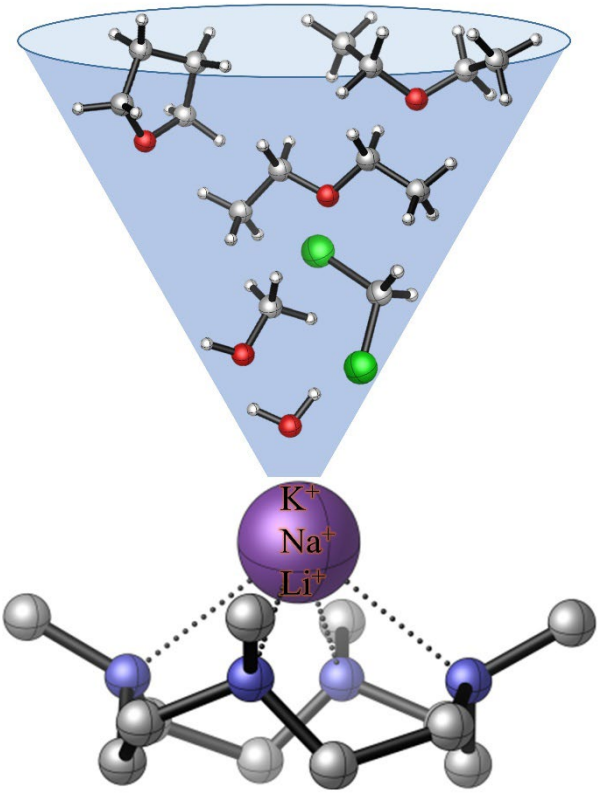

Abstract

Metal-cyclen complexes have a number of important applications. However, the coordination chemistry between metal ions and cyclen-based macrocycles is much less well studied compared to their metal ion-crown ether analogues. This work, which makes a contribution to address this imbalance by studying complex ions of the type $[M(Me_4cyclen)(L)]^+$, was initiated by results of an experimental study which prepared some Group 1 metal cyclen complexes, namely $[Li(Me_4cyclen)(H_2O)][BAr^F]$ and $[Na(Me_4cyclen)(THF)][BAr^F]$ and obtained their X-ray crystal structures [Dalton Trans., 2015, 44, 13853-13866].

The lowest $[M(Me_4cyclen)(L)]^+$ minimum energy structures (M = Li, Na, K, and L = H_2O, THF, DEE, MeOH, DCM) are studied using DFT calculations. The geometry of each $[M(Me_4cyclen)(L)]^+$ structure and, in particular, the conformation of L are found to be mainly governed by steric hindrance which decreases as the size of the ionic radius increases from $Li^+ \rightarrow Na^+ \rightarrow K^+$. Good agreement of computed geometrical parameters of $[Li(Me_4cyclen)(H_2O)]^+$ and $[Na(Me_4cyclen)(THF)]^+$ with the corresponding geometrical parameters derived from the crystal structures $[Li(Me_4cyclen)(H_2O)]^+[BAr^F]^-$ and $[Na(Me_4cyclen)(THF)]^+[BAr^F]^-$ is obtained. Bonding analysis indicates that the stability of the $[M(Me_4cyclen)(L)]^+$ structures originates mainly from ionic interaction between the Me_4cyclen/L ligands and the M^+ centers.

The experimental observation that $[M(Me_4cyclen)(L)]^+[BAr^F]^-$ complexes could be prepared in crystalline form for $M^+ = Li^+$ and Na^+, but that experiments aimed at synthesising the corresponding K^+, Rb^+ and Cs^+ complexes failed resulting in formation of $[Me_4cyclenH][BAr^F]$ is investigated using DFT and explicitly correlated calculations, and explained by considering production of $[Me_4cyclenH]^+$ by a hydrolysis reaction, involving traces of water, which competes with $[M(Me_4cyclen)(L)]^+$ formation. $[Me_4cyclenH]^+$ formation dominates for $M^+ = K^+$, Rb^+ and Cs^+ whereas formation of $[M(Me_4cyclen)(L)]^+$ is energetically favoured for $M^+ = Li^+$ and Na^+.

The results indicate that the number and type of ligands, play a key role in stabilising the $[M(Me_4cyclen)]^+$ complexes and it is hoped that this work will encourage experimentalists to prepare and characterise other $[M(Me_4cyclen)(L)]^+$ complexes.

Keywords

DFT, alkali metal, Me_4cyclen, bond dissociation energy, DF-LCCSD(T)-F12

1.0 Introduction

Alkali metal ions are prevalent in various aspects of life on earth, in the oceans and within biological systems.[1-3] 1,4,7,10-Tetraazacyclododecane, cyclen **1a** (Scheme 1), is one of the smallest *N*-donor analogues of crown ether, which can be easily derivatised by *N*-ligating sidearm groups.[4] Its usefulness in molecular sensing, catalysis, chirality signaling, and biomedicine, has made cyclen derivatives attractive alternative hosts to crown ethers.[5-9] However, the coordination chemistry between alkali metal ions and cyclen-based macrocycles[5,10-18] is less well studied compared to their crown ether analogues.

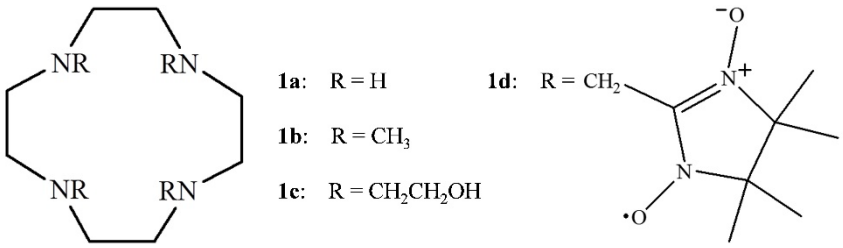

Scheme 1: Cyclen **1a** and some *N*-functionalised analogues **1b**-**d**.

Recently, as part of a study of a group of aza-macrocycles of Group 1 metal cations, some of us[17] reported the synthesis as well as the NMR and X-ray characterisation of the Li^+ and Na^+ complexes of 1,4,7,10-tetramethyl-1,4,7,10-tetraazacyclcododecane, Me4cyclen **1b** (Scheme 1), namely [Li(Me4cyclen)(H_2O)][BAr^F] and [Na(Me4cyclen)(THF)][BAr^F] (THF = tetrahydrofuran; BAr^F = tetrakis{3,5-bis(trifluoromethyl)phenyl}borate). The crystal structures show a five coordinate square pyramidal cation, consisting of four *N*-atoms from the tetradentate macrocycle and one apical *O*-donor ligand, where the auxiliary *O*-donor ligand, H_2O or THF, occupies one of the exposed coordination sites of the metal centre above the macrocycle. However, attempts to synthesise the corresponding K^+, Rb^+, and Cs^+ complexes failed and resulted in the formation of [Me4cyclenH][BAr^F]. This was an unexpected outcome although K^+ complexes of cyclen derivatives **1c** and **1d** (Scheme 1) have been synthesised.[10,11]

We were intrigued by the successful syntheses of the Li^+ and Na^+ complexes of Me4cyclen[17] but the unsuccessful synthesis of a K^+-Me4cyclen complex, and this motivated us to look into possible factors which influence the formation and stability of alkali metal complexes of Me4cyclen. Further, recent literature highlights the point that successful preparation and isolation of metal complexes can be attributed to the presence of residual coordinating solvents which can impart significant stability to the structure.[19] In this context, it is unclear how the nature of the ligand (L) coordinated above the metal in the

$[M(Me_4cyclen)]^+$ cation contributes to the overall stability of the complex $[M(Me_4cyclen)(L)]^+$. In this work, the formation and stability of $[M(Me_4cyclen)(L)]^+$ is investigated using density functional theory (DFT) calculations, by studying the effect of coordinating commonly used *O*-donor solvents, namely H_2O, THF, diethyl ether (DEE), and methanol (MeOH) to $[M(Me_4cyclen)]^+$ (M = Li, Na, K). The fact that weakly coordinating polar dichloromethane (DCM) was used as a solvent during the successful syntheses of Li^+ and Na^+ complexes,[17] encouraged us to include L = DCM in this study.

The aim of this work, therefore, is to gain some insight into why $[Li(Me_4cyclen)(H_2O)][BAr^F]$ and $[Na(Me_4cyclen)(THF)][BAr^F]$ could be prepared but experiments aimed at synthesising the corresponding K^+, Rb^+ and Cs^+ complexes failed and resulted in formation of $[Me_4cyclenH][BAr^F]$. Competing hydrolysis from traces of water has been suggested as a likely cause of preferential formation of $[Me_4cyclenH][BAr^F]$ for K^+, Rb^+ and Cs^+.[17] To achieve this, the following computational strategy was adopted:-

(a) Minimum energy geometries were computed for (i) $[M(Me_4cyclen)(L)]^+$, (ii) $[M(Me_4cyclen)]^+$, (iii) $[M^+\text{-}L]$, and (iv) $[Me_4cyclenH]^+$. Their electronic structures were investigated by inspection of the converged wavefunctions and the natural charges on each centre.

b) For the two compounds $[Li(Me_4cyclen)(H_2O)][BAr^F]$ and $[Na(Me_4cyclen)(THF)][BAr^F]$ where X-ray crystal structures are available, the geometrical parameters computed with DFT calculations were compared with the X-ray experimental parameters.

c) The dissociation energy of the ligand (L) from each $[M(Me_4cyclen)(L)]^+$ ion was computed using DFT calculations for M = Li, Na, K, and L = H_2O, THF, DEE, MeOH, DCM. Improved dissociation energies were obtained using single-point DF-LCCSD(T)[20] and explicitly correlated DF-LCCSD(T)-F12[21] calculations.[18,22,23]

(d) Then, in order to investigate formation of $[Me_4cyclenH]^+$ and $[M(Me_4cyclen)(L)]^+$, reaction energies were computed using these methods for the two competing reactions which form these ions:-

(A) $H_3O^+ + [Me_4cyclen] + L \rightarrow [Me_4cyclenH]^+ + H_2O + L$

(B) $M^+ + [Me_4cyclen] + L \rightarrow [M(Me_4cyclen)]^+ + L \rightarrow [M(Me_4cyclen)(L)]^+$

e) Calculations were then performed on some other metal-cyclen complexes where experimental structures are available, i.e. **1c**, **1d** (see Scheme 1) and $[K(Me_4cyclen)]^+[HBPh_3]^-$ complex [24] ($[HBPh_3]^-$ = hydridotriphenylborate), to make a comparison with the structure and bonding in the $[M(Me_4cyclen)(L)]^+$ complexes.

2.0 Computational Details

The DFT functionals BP86[25] and B3LYP[26] were used to perform geometry optimisations for all the chemical species investigated in this work.[27,28] The 6-311G(d,p) basis set[29] was employed for the atoms. The functionals were selected, with the 6-311G(d,p) basis set, based on results of our recent studies on alkali metal ion-macrocyclic complexes.[17,18,30] Geometry optimisation was followed by analytic Hessian computation at the same levels of theory, and the absence of negative Hessian eigenvalues confirmed the stationary points as minima on the potential energy hypersurfaces. Bond dissociation energies (BDEs) were calculated for the process, $[M(Me_4cyclen)(L)]^+ \rightarrow [M(Me_4cyclen)]^+ + L$ and reaction energies (ΔEs) were calculated for reactions (A) and (B), where M = Li, Na, K, and L = H_2O, THF, DEE, MeOH, DCM, using these functionals with the 6-311G(d,p) basis set.[31] Basis set superposition error (BSSE) correction, as implemented by the Boys-Bernardi counterpoise method,[32] and zero-point energy (ZPE) correction were included in the BDEs and ΔEs. Reported relative energies are given at 298.15 K and 1 atm. All density functional computations were performed using the Gaussian 09 package.[33] Natural bond orbital (NBO) analysis[34,35] was also carried out using the NBO program as implemented in the Gaussian 09 package.[36] Throughout this work, $[M(Me_4cyclen)(L)]^+$ structures optimised with the BP86 functional are denoted **M-L-1a** and those optimised with the B3LYP functional are denoted **M-L-2a**.

High level *ab initio* methods were employed to assess the performance of the DFT calculations and to obtain more reliable BDEs and ΔEs.[18,22,23] Single-point DF-LCCSD(T)[20] and explicitly correlated DF-LCCSD(T)-F12x (x = a, b)[21] calculations were performed at the BP86/6-311G(d,p) and B3LYP/6-311G(d,p) lowest minimum energy geometries of $Me_4cyclen$, $[M(Me_4cyclen)]^+$, $[M(Me_4cyclen)(L)]^+$, L, $[Me_4cyclenH]^+$, H_2O and H_3O^+ using the MOLPRO 2010.1[37] and 2015.1 program.[38] All DF-LCCSD(T) and DF-LCCSD(T)-F12x calculations were preceded by a density fitted Hartree-Fock (HF) calculation.[39] The local correlation methods together with the density fitting (DF) approximation allow the efficient treatment of larger molecules. The inclusion of explicitly correlated terms accounts for basis set incompleteness and domain approximation associated errors.[20,21] Further details of the DF-LCCSD(T) and DF-LCCSD(T)-F12x calculations are given in the Supplementary Information.

All computations were carried out with resources (CPU time and software) provided by the GridChem Science Gateway,[40-42] the UK National Service for Computational Chemistry Software (NSCCS) and a local cluster in Hong Kong. The processing of input and output files was carried out using ExcelAutomat.[43]

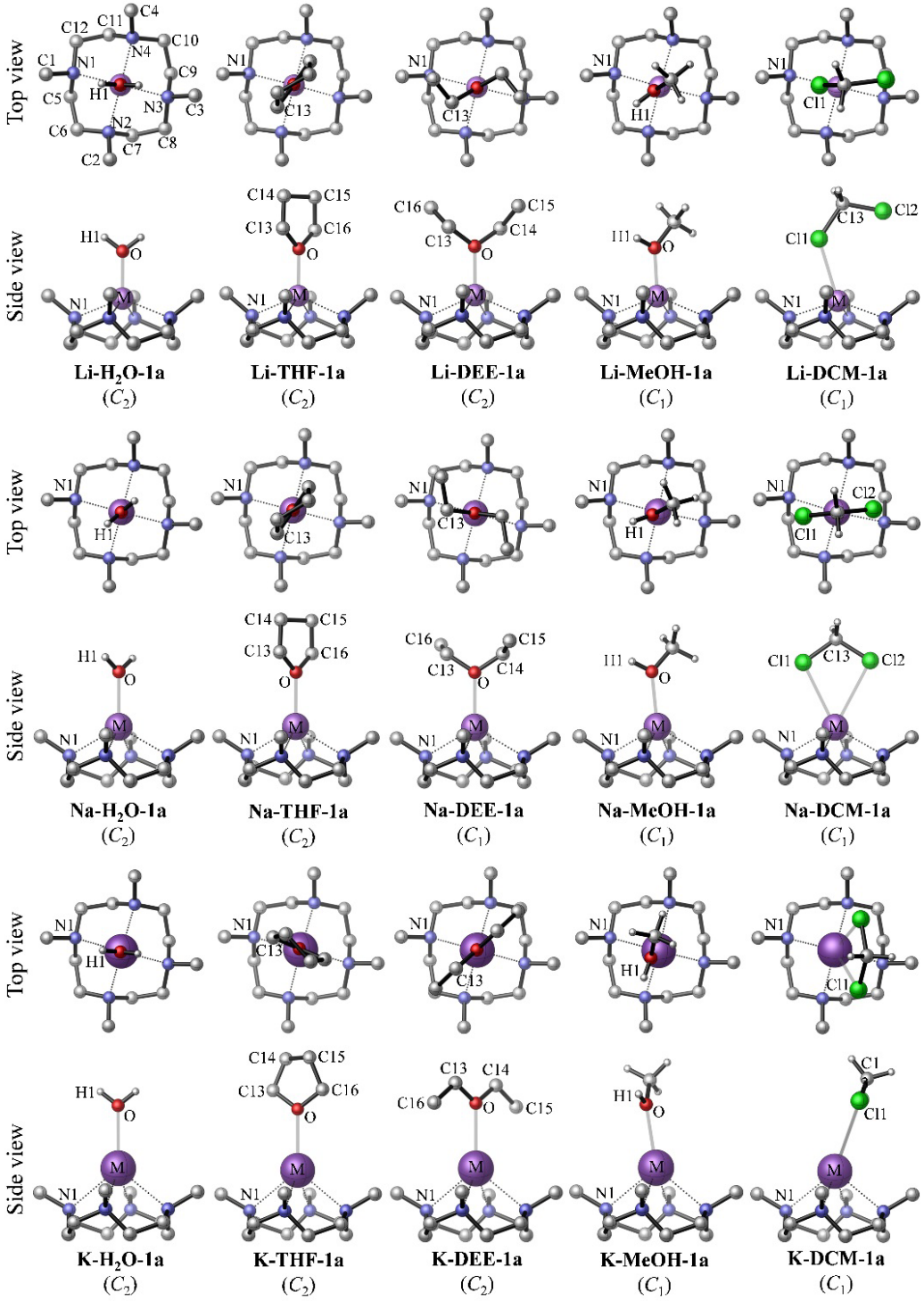

Figure 1: Lowest $[M(Me_4cyclen)(L)]^+$ minimum energy structures obtained using the BP86/6-311G(d,p) method. The symmetry of each structure is provided. Selected H atoms are omitted for clarity.

3.0 Results and Discussion

3.1 Geometries and Electronic Structures of (i) [M(Me$_4$cyclen)(L)]$^+$, (ii) [M(Me$_4$cyclen)]$^+$, (iii) [M$^+$-L], and (iv)[Me$_4$cyclenH)]$^+$.

The lowest minimum energy structures obtained using the BP86/6-311G(d,p) method for [M(Me$_4$cyclen)(L)]$^+$ and [M(Me$_4$cyclen)]$^+$ are shown in Figures 1 and 2, respectively. Selected geometrical parameters for these structures are shown in Tables S2 and S1. The computed BP86/6-311G(d,p) structure of [Me$_4$cyclenH]$^+$ is shown in Figure 3 with selected geometrical parameters given in Table S16. The corresponding structures and geometrical parameters of [M$^+$-L] are shown in Figure S8 and Table S4. In all cases, very similar geometrical parameters were obtained with both the BP86 and B3LYP functionals.

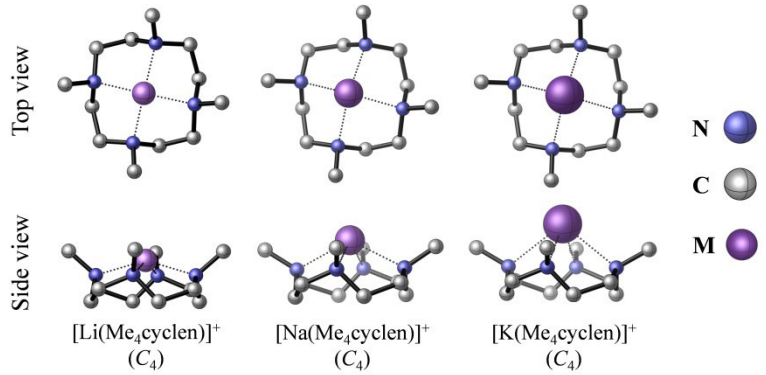

Figure 2: Optimised lowest energy structures of [M(Me$_4$cyclen)]$^+$ obtained using the BP86/6-311G(d,p) method. The symmetry of each structure is provided. All H atoms are omitted for clarity.

The overall changes observed in the geometrical parameters upon complexation of [M(Me$_4$cyclen)]$^+$ to L indicate that (i) the effects of steric hindrance between Me$_4$cyclen and L are maximum in **Li-DEE-1a** (**Li-DEE-2a**), (ii) DCM coordinates weakly to the [M(Me$_4$cyclen)]$^+$ unit as compared to its *O*-donor analogues, and (iii) as the size of the ionic radius of M$^+$ increases from Li$^+$ → Na$^+$ → K$^+$, steric hindrance between Me$_4$cyclen and L in **M-L-1a** (**M-L-2a**) decreases, and thus the effect on the geometry of the [M(Me$_4$cyclen)]$^+$ unit in [M(Me$_4$cyclen)(L)]$^+$ also decreases

An analysis of the lowest minimum energy structures with *O*-donor ligands reveals that the M–O bond of **M-L-1a** (**M-L-2a**), for L = H$_2$O, THF, and DEE, is essentially normal to the plane formed by the four *N*-donor atoms of Me$_4$cyclen, with the dipole moment of each structure aligning along the M–O bond. The M–O bond of **M-MeOH-1a** (**M-MeOH-2a**) is tilted by ≈ 3-10° from the normal of the equatorial plane. In general, the M–O bond distances of **M-H$_2$O-1a** (**M-H$_2$O-2a**), **M-THF-1a** (**M-THF-2a**), **M-DEE-1a** (**M-DEE-2a**), and **M-MeOH-1a** (**M-MeOH-2a**) are comparable (for M = Li and Na; see Tables 1 and S2). The K–O bond distance of **K-DEE-1a** (BP86, 2.805 Å; B3LYP, 2.788 Å) is significantly longer than

the K–O bonds in **K-H_2O-1a** (BP86, 2.718 Å; B3LYP, 2.711 Å), **K-THF-1a** (BP86, 2.721 Å; B3LYP, 2.705 Å), and **K-MeOH-1a** (BP86, 2.729 Å; B3LYP, 2.713 Å). This observation can be correlated to the spatial arrangement of the DEE fragment in the complexes. The **M-DEE-1a** (**M-DEE-2a**) structures (for M = Li and Na) have their DEE fragment in a gauche-gauche (GG) conformation while for M = K, **K-DEE-1a** (**K-DEE-2a**) adopts a trans-trans (TT) conformation. The M–N and M–O bond distances of **K-DEE-1a** (**K-DEE-2a**) are longer than their Li^+ and Na^+ counterparts, thus its DEE framework is free to adopt a less sterically hindered conformation, a TT conformation. This is consistent with the known lowest energy structure of DEE in the gas-phase which is known to be TT[44,45] and the results of DFT BP86 and B3LYP calculations on DEE summarised in Figures S8 and S9 (Figure S9 shows a diagram of the TT, TG, and GG structures of DEE). Further details of the results of the calculations carried out on the $[M(Me_4cyclen)(L)]^+$ and $[M(Me_4cyclen)]^+$ ions are given in the SI.

A reasonable description of the electronic structures of the **M-L-1a** (**M-L-2a**) $[M(Me_4cyclen)(L)]^+$ ions can be obtained from NBO analysis and from inspection of the converged wavefunctions. The natural charges on selected centres of the optimised (a) free Me_4cyclen and L ligands, (b) $[M(Me_4cyclen)]^+$, (c) $[M^+$-L], (d) **M-L-1a** (**M-L-2a**) and (e) $[Me_4cyclenH]^+$ structures are given in Tables S7-10, S17. Coordination of L to M^+ results in a slight drop of the positive charge on the cation (from +1.0). Taking the computed charge densities on M in $[M^+$-L] for M = Na as examples, values obtained were +0.99, +0.98, +0.97, +0.98, and +0.94 for L = H_2O, THF, DEE, MeOH, and DCM (see Table S8). For the *O*-containing ligands, the charge on the O atom coordinated to the metal becomes more negative on forming $[M^+$-L] in all cases. For example, in THF, the negative charge on the O atom increases from -0.57 in THF to -0.71 in $[Na^+$-THF] (BP86 charge densities are quoted above but the B3LYP values are very similar). Also, the negative charges on the carbon atoms of the THF show virtually no change but the positive charges on the hydrogen atoms increase on going from THF to $[Na^+$-THF]. This is consistent with charge transfer taking place from the ligand O atom to the metal and then electron density being transferred to the O atom within the ligand via the σ O–C, σ C–C, and σ C–H bonding orbitals of THF. In the case of L = DCM, a similar picture holds with the charge on the carbon atom becoming less negative and the charge of the hydrogen atoms becoming more positive on forming $[M^+$-L]. Again on forming $[M^+$-L], charge transfer occurs from Cl to M^+ accompanied by electron density transfer to the Cl atoms from within the ligand via the σ C–Cl and σ C–H bonding orbitals. For M = Na and K, where the metal is bonded to two chlorine atoms, the Cl atoms show a

slight increase of negative charge whereas for M = Li, where the metal is bonded to one Cl atom, this Cl atom shows a slight decrease of negative charge on going from M^+ + L to [M^+-L].

Coordination of M^+ to Me_4cyclen to give [M(Me_4cyclen)]$^+$ shows similar trends. The positive charge on the metal drops from +1.0 to +0.69, +0.79, and +0.87 for Li^+, Na^+, and K^+. Also the charge on the nitrogen atoms coordinated to the metal becomes more negative (see Table S7). Upon complexation of M^+ to Me_4cyclen, electron density is transferred from the N 2p non-bonding orbitals of the Me_4cyclen ring to the metal, with electron density then being transferred to the N atoms from the σ C–N, σ C–C, and σ C–H bonding orbitals. The negative charges on the carbon atoms in Me_4cyclen show only small changes but the positive charges on the hydrogen atoms of the CH_2 as well as the CH_3 units in the macrocycle increase.

Addition of a solvent, L, to [M(Me_4cyclen)]$^+$ to give [M(Me_4cyclen)(L)]$^+$ gives rise to further electron transfer to the metal and hence, a reduced metal positive charge. As observed for the M^+ + L → [M^+-L] process, the negative charge on the O atom (of the *O*-containing solvents) increases, the negative charges on the carbon atoms of the solvent show only small changes and the positive charges on the H atoms of the solvent increase. Electron transfer takes place from the O atom to the metal accompanied by electron transfer to the O atom from the σ O–C, σ C–C, and σ C–H bonding orbitals of the ligand. Similar trends are observed in the L = DCM case.

A comparison of the *O*-containing [M^+-L] complexes shows that the O atoms of [M^+-H_2O] are the most negatively charged while its M^+ centres are the most positively charged with natural charges in the order of [M^+-H_2O] > [M^+-MeOH] > [M^+-THF] > [M^+-DEE]. A similar trend occurs for the corresponding **M-L-1a** (**M-L-2a**) structures, indicating less electron density being transferred from H_2O to M^+ with respect to the THF, DEE, and MeOH ligands, consistent with the known order of first adiabatic ligand ionisation energies of H_2O > MeOH > THF > DEE.[46] More electron density is transferred from the Cl atoms to the M^+ centres in both the [M^+-DCM] and **M-DCM-1a** (**M-DCM-2a**) structures than for the *O*-containing solvents, as indicated by the lower positive charges on the M^+ centres for L = DCM compared to that of the *O*-containing analogues. The lower electronegativity of the Cl atom with respect to the O atom[47] is consistent with the higher transfer of electron density to the M^+ centres. A similar observation has been made in a study of the bonding characters of [Ag^+-DCM] and [Ag^+-OSO], where the DCM and SO_2 ligands interact with Ag^+ via bidentate η^2-Cl,Cl and monodentate η^1-O coordination modes, respectively.[48]

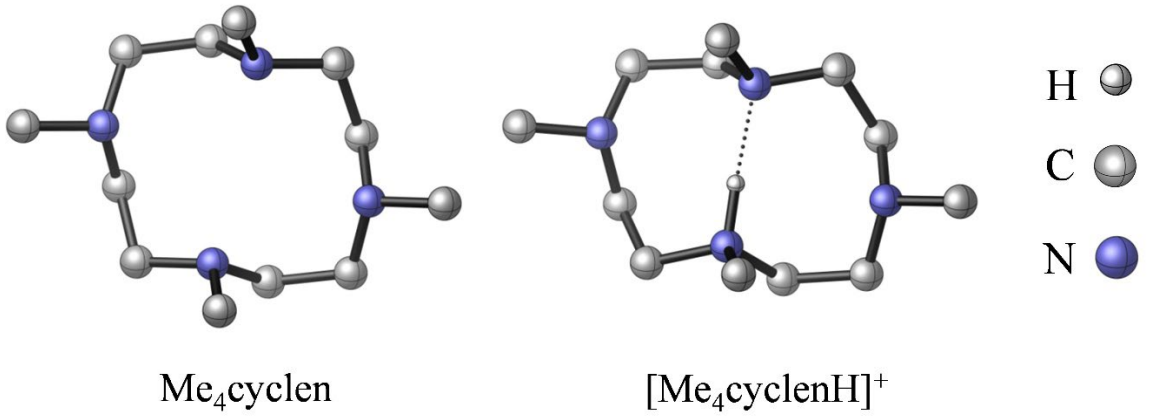

Figure 3: Optimised Me4cyclen and $[Me_4cyclenH]^+$ structures obtained using the BP86/6-311G(d,p) method. Selected H atoms are omitted for clarity.

On considering the steps in reaction (B) M^+ + Me4cyclen → $[M(Me_4cyclen)]^+$ and $[M(Me_4cyclen)]^+ + L \rightarrow [M(Me_4cyclen)(L)]^+$, significantly more electron density is transferred to the metal in the first step than the second step. This implies that M^+ is more tightly bound to Me4cyclen than L in the **M-L-1a** (**M-L-2a**) $[M(Me_4cyclen)(L)]^+$ complexes. Also, the M^+ centres accept less electron density as the radius of the M^+ ion increases from $Li^+ \rightarrow Na^+ \rightarrow K^+$ and the first ionisation energy of M decreases from Li → Na → K. In general, the NBO analysis indicates that the metal-ligand bonding in the $[M(Me_4cyclen)]^+$, $[M^+\text{-L}]$, and **M-L-1a** (**M-L-2a**) $[M(Me_4cyclen)(L)]^+$ complexes is mainly ionic in nature.

Formation of $[Me_4cyclenH]^+$ occurs via addition of a proton to Me4cyclen via reaction (A). The computed BP86/6-311G(d,p) minimum energy structure is shown in Figure 3, selected geometrical parameters for this structure are shown in Table S16 and the natural charges on selected centres are shown in Table S17. Addition of H^+ to Me4cyclen to form $[Me_4cyclenH]^+$ results in a structure with the proton attached to one nitrogen atom inside the cyclen ring (see Figure 3) with a N-H distance of 1.10 Å (BP86/6-311G(d.p) value), and electron transfer occurs from nitrogen atoms to the hydrogen accompanied by electron transfer to the nitrogen atoms from the σ orbitals of the cyclen unit. The charge on the hydrogen atom drops from +1.0 (in H^+) to +0.50 in the complex, with the C and N atoms of the cyclen ring becoming more negatively charged and the cyclen hydrogen atoms becoming more positively charged (see Table S17).

Computed harmonic IR spectra together with selected vibrational modes for the $[M^+\text{-L}]$, $[M(Me_4cyclen)]^+$, $[M(Me_4cyclen)(L)]^+$, Me4cyclen and $[Me_4cyclenH]^+$ minimum energy

structures, obtained using the BP86/6-311G(d,p) method, are provided in Figures S11-S13, S20 and Tables S11-S13, S18. These should be useful in future experimental work to prepare and study these complexes.

3.2 Comparison of the computed geometrical parameters with the experimental parameters for the two compounds where X-ray crystal structures are available, [Li(Me$_4$cyclen)(H$_2$O)][BAr^F] and [Na(Me$_4$cyclen)(THF)][BAr^F].

[Li(Me$_4$cyclen)(H$_2$O)]$^+$ and [Na(Me$_4$cyclen)(THF)]$^+$ are the two [M(Me$_4$cyclen)(L)]$^+$ ions for which X-ray crystal structures have been obtained.[17] [Li(Me$_4$cyclen)(H$_2$O)][BAr^F] was prepared by reaction of [Li(H$_2$O)$_4$][BAr^F] with Me$_4$cyclen in DCM. Similarly, reaction of Me$_4$cyclen with Na[BAr^F].2THF in DCM yielded [Na(Me$_4$cyclen)(THF)][BAr^F]. Clearly, the presence of H$_2$O or THF in the crystal structures arises from the [Li(H$_2$O)$_4$][BAr^F] and Na[BAr^F].2THF salts used, respectively. It is noteworthy that no evidence of coordination of DCM (or *n*-hexane, the other solvent used in these syntheses) to the [M(Me$_4$cyclen)]$^+$ ion was observed. Also, attempts to synthesise the [M(Me$_4$cyclen)(L)][BAr^F] salts for M = K, Rb, and Cs were unsuccessful resulting only in isolation of [Me$_4$cyclenH][BAr^F].[17]

The computed geometrical parameters, for **Li-H$_2$O-1a** (**Li-H$_2$O-2a**) and **Na-THF-1a** (**Na-THF-2a**), are compared with the corresponding geometrical parameters obtained from the crystal structures[17] in Table 1. In general, the agreement between computed and experimental parameters is good. The BP86 M–N bond distances are all slightly higher and the BP86 N–M–N bond angles are all slightly lower than the experimental values. This is also true of the B3LYP computed geometrical parameters. In general, the computed and experimentally derived structures are comparable with differences of < 0.110 Å in M–N bond distances, < 2.5° in N–M–N bond angles, and < 3.5° in N–C–C–N dihedral angles (Table 1).

Table 1: Selected geometrical parameters of the lowest [M(Me$_4$cyclen)(L)]$^+$ minimum energy structures obtained using the BP86/6-311G(d,p) method for M = Li, Na, and K with L = H$_2$O and THF.

	M-H$_2$O-1a				**M-THF-1a**			
Bond distances (Å)	Li	Expt.[a]	Na	K	Li	Na	Expt.[a]	K
M–N1	2.256	2.186(8)	2.502	2.842	2.253	2.521	2.463(4)	2.853
M–N2	2.254	2.206(8)	2.505	2.835	2.330	2.522	2.461(3)	2.843
M–N3	2.256	2.179(8)	2.502	2.842	2.253	2.521	2.453(4)	2.853
M–N4	2.254	2.154(9)	2.505	2.835	2.330	2.522	2.444(4)	2.843
M–O	2.009	1.98(1)	2.340	2.718	2.028	2.351	2.244(3)	2.721

Bond angles (°)								
N1–M–N2	82.3	82.8(3)	75.9	66.9	80.9	75.3	75.4(1)	66.8
N2–M–N3	82.4	82.1(3)	76.2	66.9	81.6	75.6	75.6(1)	66.7
N3–M–N4	82.3	84.7(3)	75.9	66.9	80.9	75.3	76.0(1)	66.8
N4–M–N1	82.4	82.6(3)	76.2	66.9	81.6	75.6	75.5(2)	66.7
Torsion (°)								
N1–C5–C6–N2	-57.1	59.4(7)	-61.9	-64.7	-56.1	-62.2	-64(1)	-64.9
N2–C7–C8–N3	-57.1	55.8(8)	-62.6	-64.2	-59.9	-62.7	-61(1)	-64.4
N3–C9–C10–N4	-57.1	54.0(9)	-61.9	-64.7	-56.1	-62.2	-59(1)	-64.9
N4–C11–C12–N1	-57.1	57.5(7)	-62.6	-64.2	-59.9	-62.7	-65(1)	-64.4
N1–M–O–H1	11.7	–	55.3	10.1	–	–	–	–
N1–M–O–C13	–	–	–	–	69.1	70.0	59.6	-7.7

[a] Corresponds to the $[Li(Me_4cyclen)(H_2O)]^+$ and $[Na(Me_4cyclen)(THF)]^+$ crystal structures, respectively.[17]

3.3 Computed bond dissociation energies (BDEs) of the ligand (L) from each $[M(Me_4cyclen)(L)]^+$ ion, for M = Li, Na, K, and L = H_2O, THF, DEE, MeOH, DCM.

BDEs for the process $[M(Me_4cyclen)(L)]^+ \rightarrow [M(Me_4cyclen)]^+ + L$ were calculated using the DFT method with the BP86 and B3LYP functionals and the 6-311G(d,p) basis set. More reliable values were obtained using high level single-point DF-LCCSD(T) and DF-LCCSD(T)-F12x calculations at the BP86 and B3LYP optimised geometries. The calculated BP86 and the corresponding DF-LCCSD(T) and DF-LCCSD(T)-F12x BDEs for BP86 **M-L-1a** minimum energy structures are presented in Table 2 while BDEs derived for the B3LYP **M-L-2a** minimum energy structures are shown in Table S14. The BDE values obtained will provide insight into the choice of appropriate solvent/s to be used for the synthesis of the **M-L-1a** (**M-L-2a**) complexes and may further aid in controlling the product composition (*via* removal/addition of appropriate solvents which are Lewis bases).[19] As can be seen in Tables 2 and S14, the BP86 and B3LYP BDEs are consistent, with the B3LYP BDEs being always slightly higher than the BP86 values. The single-point higher level calculations provide more reliable BDEs than the DFT values. The DF-LCCSD(T) and DF-LCCSD(T)-F12x BDEs, obtained using both the double and triple-ζ quality basis sets, are comparable to each other. However, they are significantly higher than the BSSE corrected DFT BDE values, with differences in the region of 6-40 $kJ.mol^{-1}$ being observed.

Table 2: Calculated bond dissociation energies ($kJ.mol^{-1}$) of the lowest **M-L-1a** minimum energy structures.

	BP86/6-311G(d,p)	DF-LCCSD(T)/nZ//	DF-LCCSD(T)-F12x[a]/nZ-F12 //BP86/6-311G(d,p)

	ΔE^{ZPE}	$\Delta E^{ZPE+BSSE}$	BP86/6-311G(d,p) n = D	BP86/6-311G(d,p) n = T	n = D x = a	n = D x = b	n = T x = a	n = T x = b
Li-H_2O-1a	64.3	39.7	56.6	59.1	59.3	59.5	60.1	60.3
Li-THF-1a	56.3	43.1	71.6	74.3	76.8	77.3	77.2	77.4
Li-DEE-1a	34.3	21.6	67.3	57.9	59.7	60.2	61.7	61.9
Li-MeOH-1a	58.0	40.1	60.0	64.0	64.8	65.1	65.6	65.8
Li-DCM-1a	12.6	6.6	32.6	32.1	33.6	33.9	34.2	34.4
Na-H_2O-1a	67.2	45.3	51.1	57.5	55.5	55.7	57.5	57.6
Na-THF-1a	63.9	52.1	64.6	67.0	70.6	70.8	70.6	70.7
Na-DEE-1a	46.4	35.1	50.0	52.7	56.4	56.7	55.7	55.8
Na-MeOH-1a	62.2	46.5	56.5	60.2	60.0	60.1	59.6	59.5
Na-DCM-1a	21.7	15.8	38.2	39.5	40.2	40.5	39.3	39.3
K-H_2O-1a	55.0	39.0	42.1	43.0	43.7	43.8	45.3	45.5
K-THF-1a	52.8	44.2	53.3	50.0	51.2	51.1	51.1	51.3
K-DEE-1a	39.7	31.1	54.4	51.4	51.1	51.1	53.4	53.5
K-MeOH-1a	49.9	38.4	45.3	45.5	45.3	45.2	46.9	47.0
K-DCM-1a	19.4	15.5	32.6	32.8	31.5	31.5	33.2	33.3

[a] The 3*A ansatz in conjunction with the (Fix,NoX) options was used; the MOLPRO default option is (Loc,Fix); see SI section.

The **M-DCM-1a** (**M-DCM-2a**) structures have lower BDEs than their *O*-containing analogues. These lower BDEs are representative of the weak interaction between DCM and $[M(Me_4cyclen)]^+$ and this correlates with the M–Cl bond distances in the DCM complexes being much longer than the M–O bond distances in the *O*-donor ligand complexes (Table S2). This is also consistent with the fact that DCM was used during the synthesis of the alkali metal-Me_4cyclen complexes, $[Li(Me_4cyclen)(H_2O)][BAr^F]$ and $[Na(Me_4cyclen)(THF)][BAr^F]$, but was not incorporated as a ligand into the product crystals obtained. For M = Li and Na, the **M-L-1a** (**M-L-2a**) structures have DF-LCCSD(T) and DF-LCCSD(T)-F12x BDEs in the order of L = THF > MeOH > DEE ≈ H_2O, with the strongest interaction being between THF and $[M(Me_4cyclen)]^+$. The BSSE uncorrected DFT BDEs do not follow the same trend, although the BSSE corrected values do, and this indicates the importance of BSSE correction in calculating DFT BDEs. Higher level calculations based on the BP86 lowest minimum energy structures show that the BDEs of **K-THF-1a** and **K-DEE-1a** are comparable, while those based on the B3LYP lowest minimum energy structures show that the BDE for **K-DEE-2a** is marginally greater than that of **K-THF-2a**. The trend in the DFT BDEs for the loss of *O*-donor ligands from **K-L-1a** (**K-L-2a**) is not consistent with that obtained from the higher level

calculations which are in the order of THF ≈ DEE > MeOH > H_2O. The DFT BDEs for the loss of L from the [M^+-L] structures follow a similar trend (L = THF > DEE > MeOH > H_2O > DCM; see Table S5) as that for the **K-L-1a** (**K-L-2a**) structures. The BDE values, obtained using the higher level calculations, decrease on going from $Li^+ \rightarrow Na^+ \rightarrow K^+$ for **M-L-1a** (**M-L-2a**) for a given L, where L = H_2O, THF, DEE, and MeOH, consistent with the lengthening of the M–O bond. However, the DFT BDEs do not follow the same trend. At all levels of theory, the BDEs of **Na-DCM-1a** (**Na-DCM-2a**) are higher than that of the Li^+ analogues. The bidentate η^2-Cl,Cl coordination mode between DCM and [Na(Me$_4$cyclen)]$^+$ in **Na-DCM-1a** (**Na-DCM-2a**) results in a stronger interaction compared to the monodentate η^1-Cl coordination mode between DCM and [Li(Me$_4$cyclen)]$^+$ in **Li-DCM-1a** (**Li-DCM-2a**). The BDEs of **K-DCM-1a** (**K-DCM-2a**) are lower than their Li^+ and Na^+ counterparts at the DF-LCCSD(T) and DF-LCCSD(T)-F12x levels, though with marginal differences between the BDE values of **M-DCM-1a** (**M-DCM-2a**), for M = Li and K. In contrast, the DFT BDEs for the dissociation process, [M^+-DCM] $\rightarrow$ M^+ + DCM, decrease systematically on going from $Li^+ \rightarrow Na^+ \rightarrow K^+$ (Table S5).

The dependence of the calculated BDEs on the methods and basis sets used in this work are depicted in Figures S15 and S16 (with relevant BDE values provided in Tables 2 and S14). Also, the ansatz options to be used for the DF-LCCSD(T)-F12x calculations and the basis set effects on the DF-LCCSD(T) and DF-LCCSD(T)-F12x calculations are discussed in the SI.
The main conclusions of this section are:-
(i) The geometry effects on the BDEs from the two functionals used are negligibly small, and (ii) calculations with the DF-LCCSD(T) method with a DZ basis set are inadequate, but DF-LCCSD(T)-F12x calculations with a DZ-F12 basis set are expected to be reliable and give accurate relative energies. This latter method is recommended for calculations of BDEs for the type of complexes considered in this work.

In summary, for lower level geometry optimisation calculations, some commonly used functionals, such as BP86 or B3LYP, used in the present study, appear to be adequate, while for improved relative electronic energies, the DF-LCCSD(T)-F12x method with basis sets of at least DZ-F12 quality is required.

Table 2 clearly shows (e.g. for the DF-LCCSD(T)-F12x/DZ-F12//BP86/6-311G(d,p) values) for the **M-L-1a** complexes (BP86 geometries) that for a given metal, M = Li, Na, or K, the BDE is lowest when L = DCM. Also, for a given ligand, the BDE is lowest when M = K. The same trends are observed in Table S14 for **M-L-2a** complexes (B3LYP geometries).

3.4 Reactions energies computed for reactions A and B to investigate the competitive formation of $[Me_4cyclenH]^+$ and $[M(Me_4cyclen)(L)]^+$.

In order to investigate why $[Li(Me_4cyclen)(H_2O)][BAr^F]$ and $[Na(Me_4cyclen)(THF)][BAr^F]$ could be prepared but experiments aimed at synthesising the corresponding K^+, Rb^+ and Cs^+ complexes failed and resulted in formation of $[Me_4cyclenH][BAr^F]$, reaction energies (ΔEs) for reactions A and B, which form $[Me_4cyclenH]^+$ and $[M(Me_4cyclen)(L)]^+$ respectively, were computed at the same levels as used in the previous section to calculate **M-L-1a** BDEs (see Table 2). It should be noted that, as written, reaction (B) is a two step process.

Table 3: Calculated reaction energies ($kJ.mol^{-1}$) of the reactions A and B.

(A) $H_3O^+ + [Me_4cyclen] + L \rightarrow [Me_4cyclenH]^+ + H_2O + L$

(B) $M^+ + [Me_4cyclen] + L \rightarrow [M(Me_4cyclen)]^+ + L \rightarrow [M(Me_4cyclen)L]^+$

		BP86/6-311G(d,p)		DF-LCCSD(T)/nZ //BP86/6-311G(d,p)		DF-LCCSD(T)-F12x[a]/nZ-F12 //BP86/6-311G(d,p)			
		ΔE^{ZPE}	$\Delta E^{ZPE+BSSE}$	n = D	n = T	n = D		n = T	
						x = a	x = b	x = a	x = b
(A)		-366.7	na[b]	-405.2	-397.9	-402.7	-402.0	-399.1	-398.5
(B)	**Li-H_2O-1a**	-496.8	-454.1	-496.1	-518.8	-511.4	-511.7	-519.7	-519.0
	Li-THF-1a	-488.8	-457.6	-511.1	-534.0	-529.0	-529.6	-536.8	-536.1
	Li-DEE-1a	-466.8	-436.1	-506.8	-517.6	-511.8	-512.5	-521.3	-520.6
	Li-MeOH-1a	-490.5	-454.6	-499.6	-523.6	-516.9	-517.3	-525.2	-524.5
	Li-DCM-1a	-445.1	-421.1	-472.1	-491.8	-485.8	-486.1	-493.7	-493.1
(B)	**Na-H_2O-1a**	-388.0	-346.3	-375.9	-397.0	-389.6	-389.4	-398.3	-397.6
	Na-THF-1a	-384.7	-353.1	-389.5	-406.6	-404.6	-404.4	-411.3	-410.8
	Na-DEE-1a	-367.2	-336.1	-374.8	-392.2	-390.5	-390.3	-396.5	-395.8
	Na-MeOH-1a	-383.0	-347.5	-381.3	-399.7	-394.1	-393.8	-400.3	-399.6
	Na-DCM-1a	-342.5	-316.9	-363.0	-379.0	-374.3	-374.2	-380.0	-379.4
(B)	**K-H_2O-1a**	-285.5	-255.7	-279.4	-284.7	-293.2	-293.3	-294.3	-294.1
	K-THF-1a	-283.3	-260.8	-290.6	-291.6	-300.7	-300.7	-300.1	-299.9
	K-DEE-1a	-270.2	-247.8	-291.7	-293.0	-300.6	-300.7	-302.4	-302.2
	K-MeOH-1a	-280.4	-255.1	-282.6	-287.2	-294.8	-294.7	-295.9	-295.7
	K-DCM-1a	-249.9	-232.2	-269.8	-274.4	-281.0	-281.0	-282.2	-282.0

[a] The 3*A ansatz in conjunction with the (Fix,NoX) options was used; the MOLPRO default option is (Loc,Fix); see SI section.

[b] na = not appropriate

The previous section has shown that the DF-LCCSD(T)-F12x/TZ-F12//BP86/6-311G(d,p) reaction energies are expected to be the most reliable. Also, it can be seen from Tables 2 and 3 that, for a given metal M and solvent ligand L, there are only small differences (< 2 kJ.mol^{-1}) between n = D (x = a or b) and n = T (x = a or b) DF-LCCSD(T)-F12x(=a or b)/nZ-F12//BP86/6-311G(d,p) values. Taking the n = T, ΔE value for reaction (A) (mean of x = a and b is -398.8 kJ.mol^{-1}), the corresponding reaction energies for reaction (B) for M = Li are all significantly more negative. This suggests that, on energetic grounds, preparation of the Li complexes should be feasible for all the solvent ligands investigated (and it is significant that [Li(Me$_4$cyclen)(H$_2$O)][BAr^F] has been prepared). However, for M = Na only the ΔE for reaction (B) for L = THF is clearly more negative than -398.8 kJ.mol^{-1} (by ~ 12 kJ.mol^{-1}) whereas ΔE for L = DCM is more positive than -398.8 kJ.mol^{-1} by ~ 9 kJ.mol^{-1} and for L = H$_2$O, DEE, MeOH, the reaction energy of reaction (B) is very close to this reference value (within 3 kJ.mol^{-1}). Hence, of the solvent ligands investigated, THF is the most favourable and it is significant that [Na(Me$_4$cyclen)(THF)][BAr^F] has been prepared. In the case of M = K, all reaction energies for reaction (B) are more positive than -398.8 kJ.mol^{-1} (by ~ 100 kJ.mol^{-1}) and based on this evidence, it is anticipated that reaction (A), [Me$_4$cyclenH]$^+$ formation, would dominate.

Obviously, the above discussion is based purely on reaction energies. It takes no account of the role of solvation or the anion, $[BAr^F]^-$. It also does not consider the reactant concentrations, the equilibrium constants and the reaction free energies for reactions (A) and (B). Nevertheless, it is believed that the results summarised in Table 3 do identify the main factor which explains why [M(Me$_4$cyclen)(L)]$^+$ complex ions can be prepared for M = Li and Na, but for M = K, only [Me$_4$cyclenH]$^+$ ions are obtained.

3.5b Other [M(Me$_4$cyclen)]$^+$ related structures; Metal-cyclen 1c,1d structures (see Scheme 1) and [K(Me$_4$cyclen)]$^+$[HBPH$_3$]$^-$

Three crystal structures are available in the literature which can be compared with [K(cyclen)(L)]$^+$ structures.[10,11,24] Two are structures of the type [K(R$_4$cyclen)]$^+$ which consist of an octa-coordinated K$^+$ structure with four *N*-donor atoms from the cyclen backbone and four *O*-donor atoms derived (i) from four 2-hydroxyethyl groups (Scheme 1, **1c**) and (ii) from four 4,4,5,5-tetramethylimidazolin-1-oxyl-3-oxide-CH$_2$ groups (Scheme 1, **1d**) (see Figure S10). These structures are denoted K$^+$-**1c** and K$^+$-**1d**. They are notable in that they don't

incorporate a solvent ligand. Also, the metal is eight coordinate rather than five coordinate as in the $[M(Me_4cyclen)L]^+$ complexes studied in this work and this extra coordination presumably confers extra stability on the complex. DFT geometry optimisation calculations were performed on these cations with the BP86 and B3LYP functionals. Good correlation of the computed geometrical parameters with the corresponding parameters obtained from the crystal structures was obtained (Table S6). The M–N bond distances as well as the distance between the basal plane of the four *N*-donor atoms and the K^+ ion of both optimised structures are longer while their N–M–N bond angles are smaller than that of **K-L-1a** (**K-L-2a**). In K^+-**1c** and K^+-**1d**, the M–O bond distances are shorter than the corresponding M–N distances. This was also observed for the **K-L-1a** (**K-L-2a**) structures, as well as for the other **M-L-1a** (**M-L-2a**) structures, where M = Li, Na, and L = H_2O, THF, DEE, MeOH. This is consistent with the higher affinity of *O*-donor ligands towards alkali metal ions than the *N*-donor ligands. Also, a comparison of the computed geometrical parameters of **K-L-1a** (**K-L-2a**) and K^+-**1c**/K^+-**1d** with those of the parent $[K(Me_4cyclen)]^+$ complex shows that the effect of coordinating one instead of four *O*-donor ligands to the K^+ centre is moderate but significant. For example, using BP86 computed values, the K–N bonds in K^+-**1c** are ~ 0.08 Å longer and the K–N bonds in K^+-**1d** are ~ 0.16 Å longer than the **K-L-1a** values. The K–O bonds in K^+-**1c** and K^+-**1d** are also longer than the one K–O bond in each of the **K-L-1a** complexes by ~ 0.10 Å. Clearly, the number and type of *O*-donor ligands plays an important role in determining the stability of the K^+ complexes of cyclen derivatives.

As in the $\mathbf{K^+}$**-1c** and K^+-**1d** structures**,** the $[K(Me_4cyclen)]^+[HBPH_3]^-$ structure also does not include a solvent ligand. The formal coordination number of potassium in this complex is nine, with the metal bonded to the four nitrogens of the cyclen ring, the hydrogen of the B-H unit and four carbon atoms in two of the three phenyl rings (two from each ring). Again, this extra coordination must give extra stability over that in a $[K(Me_4cyclen)(L)]^+$ complex of the type studied in this work. The computed structure (Figure S21) shows good agreement with the experimental structure[24]. At the BP86/6-311G(d,p) level, K-N distances differ from the experimental values by < 0.13 Å, the K-H distance differs from the experimental value by 0.12 Å and the K-C(coord.) distances differ by < 0.10 Å (see Table S19).

4.0 Conclusions

This work, to study the structure and bonding in $[M(Me_4cyclen)(L)]^+$ complexes, was initiated by results of an experimental study which prepared some Group 1 metal cyclen complexes, namely $[Li(Me_4cyclen)(H_2O)][BAr^F]$ and $[Na(Me_4cyclen)(THF)][BAr^F]$ and obtained their X-ray crystal structures.[17] This experimental work was notable in that although reactions were carried out in DCM as the solvent (in presence of some H_2O or THF), no DCM was incorporated into the $[M(Me_4cyclen)(L)]^+$ product ions in the crystals obtained. Also, attempts to synthesise the corresponding K^+ (and Rb^+ and Cs^+) complexes failed and resulted in the formation of the $[Me_4cyclenH][BAr^F]$.

To investigate this and to understand the role of commonly used solvents, L, the DFT method was employed to study the $[M(Me_4cyclen)(L)]^+$ complexes, where M = Li, Na, K, and L = H_2O, THF, DEE, MeOH, DCM. Coordination of L to the $[M(Me_4cyclen)]^+$ fragment entails small though systematic changes in their respective optimised geometries. H_2O, THF, DEE, and MeOH bind to the M^+ centre (for Li, Na, and K) in a monodentate η^1-O coordination mode while DCM interacts in both monodentate η^1-Cl (for Li) and bidentate η^2-Cl,Cl (for Na and K) coordination modes. Computed geometrical parameters for $[Li(Me_4cyclen)(H_2O)]^+$ and $[Na(Me_4cyclen)(THF)]^+$ are compared with those derived from available crystal structures[17] and good agreement was obtained. Bonding analysis shows that the complexes are stabilised *via* mostly ionic interaction with electron density transfer from the L and Me_4cyclen ligands to mainly the vacant 2s, 3s, and 4s orbitals of Li^+, Na^+, and K^+, respectively. Single-point DF-LCCSD(T) and the explicitly correlated DF-LCCSD(T)-F12x calculations were employed to obtain accurate bond dissociation energy (BDE) for the loss of the L from $[M(Me_4cyclen)(L)]^+$. The DCM molecule is weakly bound to the $[M(Me_4cyclen)]^+$ fragment compared to the *O*-donor analogues. This is consistent with the available experimental evidence that even when DCM is used as a solvent, in the presence of THF or H_2O, in the preparation of $[M(Me_4cyclen)(L)]^+$ complexes, DCM is not present in the $[M(Me_4cyclen)(L)]^+$ ion obtained in the crystalline product. The $[M(Me_4cyclen)(L)]^+$ complexes (M = Li, Na) have BDEs in the order of THF > MeOH > DEE ≈ H_2O, while those of their K^+ analogues are in the order of THF ≈ DEE > MeOH > H_2O, with the strongest interaction being between THF and $[M(Me_4cyclen)]^+$. The BDE associated with the loss of L is lowest for the K^+ complexes and this is consistent with the unsuccessful syntheses of $[M(Me_4cyclen)(L)]^+$ complexes containing potassium. In short, for M = K the ionic bonding in $[M(Me_4cyclen)(L)]^+$ is not sufficiently large to favour formation of $[K(Me_4cyclen)(L)]^+$ over formation of $[Me_4cyclenH]^+$. This is

confirmed by calculating the energies (ΔE) of the reactions which lead to formation of $[Me_4cyclenH]^+$ and $[M(Me_4cyclen)L]^+$:-

(A) $H_3O^+ + [Me_4cyclen] + L \rightarrow [Me_4cyclenH]^+ + H_2O + L$

(B) $M^+ + [Me_4cyclen] + L \rightarrow [M(Me_4cyclen)]^+ + L \rightarrow [M(Me_4cyclen)L]^+$

This work also highlights the importance of using anhydrous conditions when preparing $[M(Me_4cyclen)(L)]^+$ complexes. Further, coordinating ligands L (such as acetonitrile, benzene, pentane, chloroform, 2-propanol, and pyridine) in $[M(Me_4cyclen)(L)]^+$ complexes are currently being investigated.

5.0 Acknowledgements

The authors acknowledge the use of the EPSRC UK National Service for Computational Chemistry Software. This work was also supported by funding provided by the Tertiary Education Commission of Mauritius (TEC). Helpful advice from Profs Bill Levason and Gill Reid (University of Southampton) is also acknowledged.

6.0 References

1. Y. Kim, T.-T. T. Nguyen, and D. G. Churchill, *In: The Alkali Metal Ions: Their Role for Life*; A. Sigel, H. Sigel, and R. K. O. Sigel, Eds., *Met. Ions Life Sci.*, Springer International Publishing, **16**, 2016, 1.
2. G. R. C. Hamilton, S. K. Sahoo, S. Kamila, N. Singh, N. Kaur, B. W. Hylanda, and J. F. Callan, *Chem. Soc. Rev*. 2015, **44**, 4415.
3. M. C.-L. Yeung and V. W.-W. Yam, *Chem. Soc. Rev*. 2015, **44**, 4192.
4. R. B. Nazarski, *In: Macrocyclic Chemistry: New Research Development*; D. W. Fitzpatrick and H. J. Ulrich, Eds., Nova Science Publishers Inc.: New York, 2010, 1.
5. S. Shinoda, *Chem. Soc. Rev*. 2013, **42**, 1825.
6. K. Hanaoka, K. Sasakura, Y. Suwanai, S. Toma-Fukai, K. Shimamoto, Y. Takano, N. Shibuya, T. Terai, T. Komatsu, T. Ueno, Y. Ogasawara, Y. Tsuchiya, Y. Watanabe, H. Kimura, C. Wang, M. Uchiyama, H. Kojima, T. Okabe, Y. Urano, T. Shimizu, and T. Nagano, *Sci. Rep*. 2017, **7**, 40227.
7. L. Wang, H. Lin, L. Ma, J. Jin, T. Shen, R. Wei, X. Wang, H. Ai, Z. Chen, and J. Gao, *Nanoscale* 2017, **9**, 4516.
8. E. M. Surender, S. J. Bradberry, S. A. Bright, C. P. McCoy, D. C. Williams, and T. Gunnlaugsson, *J. Am. Chem. Soc.* 2017, **139**, 381.
9. T. Sagami, Y. O. Tahara, M. Miyata, H. Miyakea, and S. Shinoda, *Chem. Comm*. 2017, **53**, 3967.
10. S. Buøen, J. Dale, P. Groth, and J. Krane, *J. Chem. Soc., Chem. Comm*. 1982, 1172.
11. K. Igarashi, T. Nogamia, and T. Ishida, *Chem., Comm*. 2007, 501.
12. S. Standfuss, T. P. Spaniol, and J. Okuda, *Eur. J. Inorg. Chem*. 2010, 2987.
13. H. Ito, H. Tsukube, and S. Shinoda, *Chem. Eur. J*. 2013, **19,** 3330 and references therein.
14. H. Ito and S. Shinoda, *Chemistry Open* 2014, **3**, 238 and references therein.
15. X. Zhang, J. Yin, and J. Yoon, *Chem. Rev*. 2014, **114**, 4918.

16. E. Kriemen, M. Holzapfel, E. Ruf, J. Rehbein, and W. Maison, *Eur. J. Inorg. Chem*. 2015, 5368.
17. J. M. Dyke, W. Levason, M. E. Light, D. Pugh, G. Reid, H. Bhakhoa, P. Ramasami, and L. Rhyman, *Dalton Trans*. 2015, 13853.
18. H. Bhakhoa, L. Rhyman, E. P. F. Lee, P. Ramasami, and J. M. Dyke, *Chem. Eur. J*. 2016, **22**, 4469.
19. A. Causero, G. Ballmann, J. Pahl, H. Zijlstra, C. Färber, and S. Harder, *Organometallics*, 2016, **35**, 3350.
20. H.-J. Werner and M. Schütz, *J. Chem. Phys*. 2011, **135**, 144116.
21. T. B. Adler and H.-J. Werner, *J. Chem. Phys*. 2011, **135**, 144117.
22. A. J. Achazi, L. K. S. v. Krbek, C. A. Schalley, and B. Paulus, *J. Comput. Chem*. 2016, **37**, 18.
23. E. Goll, T. Leininger, F. R. Manby, A. Mitrushchenkov, H.-J. Werner, and H. Stoll *Phys. Chem. Chem. Phys.* 2008, **10**, 3353.
24. H. Osseili, D. Mukherjee, T. P. Spaniol, and J. Okuda *Chem. Eur. J.* 2017, **23**, 1.
25. (a) A. D. Becke, *Phys. Rev. A* 1988, **38**, 3098; (b) J. P. Perdew, *Phys. Rev. B* 1986, **33**, 8822.
26. (a) A. D. Becke, *J. Chem. Phys.* 1993, **98**, 5648; (b) C. Lee, W. Yang, and R. G. Parr, *Phys. Rev. B* 1988, **37**, 785; (c) P. J. Stephens, F. J. Devlin, C. F. Chabalowski, and M. J. Frisch, *J. Phys. Chem*. 1994, **98**, 11623.
27. H. B. Schlegel, *J. Comput. Chem*. 1982, **3**, 214-218.
28. H. B. Schlegel, *In: Modern Electronic Structure Theory*; D. R. Yarkony, Ed., World Scientific Publishing: Singapore, 1995, 459.
29. W. J. Hehre, L. Radom, P. v. R. Schleyer, and J. Pople, *Ab Initio Molecular Orbital Theory*; Wiley: New York, 1986.
30. M. J. D. Champion, J. M. Dyke, W. Levason, M. E. Light, D. Pugh, H. Bhakhoa, L. Rhyman, P. Ramasami, and G. Reid, *Inorg. Chem*. 2015, **54**, 2497.
31. C. Adamo and V. Barone, *J. Chem. Phys.* 1999, **110**, 6158.
32. S. F. Boys and F. Bernardi, *Mol. Phys*. 1970, **19**, 553.
33. M. J. Frisch *et al.*, *Gaussian 09*, Revision D.01, Gaussian, Inc., Wallingford CT, 2009.
34. A. E. Reed, R. B. Weinstock, and F. Weinhold, *J. Chem. Phys*. 1985, **83**, 735.
35. A. E. Reed, L. A. Curtiss, and F. Weinhold, *Chem. Rev*. 1988, **88**, 899.
36. E. D. Glendening, A. E. Reed, J. E. Carpenter, and F. Weinhold, NBO Version 3.1, 2001, University of Wisconsin-Madison.
37. MOLPRO, version 2010.1, a package of *ab initio* programs, H.-J. Werner, P. J. Knowles, G. Knizia, F. R. Manby, M. Schütz, and others, see http://www.molpro.net
38. MOLPRO, version 2015.1, a package of *ab initio* programs, H.-J. Werner, P. J. Knowles, G. Knizia, F. R. Manby, M. Schütz, and others, see http://www.molpro.net. (Accessed September 2017)
39. R. Polly, H.-J. Werner, F. R. Manby, and P. J. Knowles, *Mol. Phys*. 2004, **102**, 2311.
40. R. Dooley, K. Milfeld, C. Guiang, S. Pamidighantam, and G. Allen, *J. Comput. Sci*. 2014, **5**, 576.
41. N. Shen, Y. Fan, and S. Pamidighantam, *J. Comput. Sci.* 2014, **5**, 576.
42. This work used the Extreme Science and Engineering Discovery Environment (XSEDE), which is supported by National Science Foundation grant number OCI-1053575.
43. J. Z. A. Laloo, N. Laloo, L. Rhyman and P. Ramasami, J. Comput. Aided Mol. Des., 2017, 31, 667-673.
44. N. Kuze, N. Kuroki, H. Takeuchi, T. Egawa, and S. Konaka, *J. Mol. Struct*. 1993, **301**, 81.
45. N. Kuze, E. Kojima, H. Fujiwara, H. Takeuchi, T. Egawa, and S. Konaka, *J. Mol. Struct*. 1996, **375**, 231.

46. K. Kimura, S. Katsumata, Y. Achiba, T. Yamazaki, and S. Iwata, *Handbook of HeI Photoelectron Spectra of Fundamental Organic Molecules. Ionization Energies, Ab Initio Assignments, and Valence Electronic Structure for 200 Molecules,* Halsted, New York, 1981.
47. J. E. Huheey, *Inorganic Chemistry: Principles of Structure and Reactivity*, New York, Harper & Row, 1983.
48. A. Decken, C. Knapp, G. B. Nikiforov, J. Passmore, J. M. Rautiainen, X. Wang, and X. Zeng, *Chem. Eur. J.* 2009, **15**, 6504.